Online Submissions: wjg.wjgnet.com
wjg@wjgnet.com
doi:10.3748/wjg.15.1966

World J Gastroenterol 2009 April 28; 15(16): 1966-1972
World Journal of Gastroenterology ISSN 1007-9327

ORIGINAL ARTICLES

In vitro and *in vivo* suppression of hepatocellular carcinoma growth by midkine-antisense oligonucleotide-loaded nanoparticles

Li-Cheng Dai, Xing Yao, Xiang Wang, Shu-Qiong Niu, Lin-Fu Zhou, Fang-Fang Fu, Shui-Xin Yang, Jin-Liang Ping

Li-Cheng Dai, Xiang Wang, Shu-Qiong Niu, Shui-Xin Yang, Huzhou Key Laboratory of Molecular Medicine, Huzhou Central Hospital, Huzhou 313000, Zhejiang Province, China
Xing Yao, Department of General Surgery, Huzhou Central Hospital, Huzhou 313000, Zhejiang Province, China
Lin-Fu Zhou, Fang-Fang Fu, Zhejiang University School of Medicine, Hangzhou 310016, Zhejiang Province, China
Jin-Liang Ping, Department of Pathology, Huzhou Central Hospital, Huzhou 313000, Zhejiang Province, China
Author contributions: Yao X, Niu SQ, Zhou LF and Wang X performed the majority of the experiments; Ping JL, Fu FF and Yang SX provided vital reagents and analytical tools; Dai LC designed the study and wrote the manuscript.
Supported by The Science and Technology Program Fund of Zhejiang Province, No. 2006C33028
Correspondence to: Li-Cheng Dai, Huzhou Key Laboratory of Molecular Medicine, Huzhou Central Hospital, Huzhou 313000, Zhejiang Province, China. dlc@hzhospital.com
Telephone: +86-572-2033020 Fax: +86-572-2033020
Received: December 12, 2008 Revised: January 19, 2009
Accepted: January 26, 2009
Published online: April 28, 2009

Abstract

AIM: To synthesize antisense oligonucleotides (ASODNs) of midkine (MK), package the ASODNs with nanoparticles, and to inhibit hepatocellular carcinoma (HCC) growth using these nanoparticles.

METHODS: HepG2 cell proliferation was analyzed *in vitro* using the 3-(4,5-dimethythiazol-2-yl)-5-(3-carboxymethoxyphenyl)-2-(4-sulfophenyl)-2Htetrazolium, inner salt assay. The *in vivo* activity of nanoparticles delivering the MK-ASODNs was analyzed by histopathological and immunohistochemical staining and quantitative real time polymerase chain reaction (PCR).

RESULTS: The *in vitro* proliferation of HepG2 cells was significantly inhibited by the nanoparticles packaged with MK-ASODNs (NANO-ASODNs). Furthermore, the NANO-ASODNs significantly inhibited the growth of HCC in the mouse model.

CONCLUSION: NANO-ASODNs can significantly suppress the growth of HCC *in vitro* and *in vivo*.

Key words: Midkine; Nanoparticles; Hepatocellular carcinoma; Inhibition; Drug delivery

Peer reviewer: Miran Kim, PhD, Liver Research Center, Rhode Island Hospital/Brown Medical School, 55 Claverick St., Providence, RI, 02903, United States

Dai LC, Yao X, Wang X, Niu SQ, Zhou LF, Fu FF, Yang SX, Ping JL. *In vitro* and *in vivo* suppression of hepatocellular carcinoma growth by midkine-antisense oligonucleotide-loaded nanoparticles. *World J Gastroenterol* 2009; 15(16): 1966-1972 Available from: URL: http://www.wjgnet.com/1007-9327/15/1966.asp DOI: http://dx.doi.org/10.3748/wjg.15.1966

INTRODUCTION

Hepatocellular carcinoma (HCC), a primary malignancy of the liver, is one of the most common tumors worldwide. The mortality rate from HCC is the third highest worldwide for any cancer-related diseases, and since the 1990s, HCC has been the cause of the second highest mortality rate due to cancer in China[1]. Globally, the 5-year survival rate of HCC is less than 5% and 598 000 HCC patients die each year[2], mainly because no satisfactory treatment is available and chemotherapy has been extremely ineffective. Recent insights into the biology of HCC suggest that certain pathways and molecular alterations are likely to play essential roles in HCC development by promoting cell growth and survival. Growth factors and the downstream signaling factors are often overexpressed in tumors and will become the targets of diagnosis or treatment.

Midkine (MK), a heparin-binding growth factor or cytokine, has been reported to be generally overexpressed in malignant tumors[3-5], whereas in normal adult tissues, MK levels are low or undetectable[6-10]. MK exhibits several cancer-related activities, including fibrinolytic, anti-apoptotic, mitogenic, transforming, angiogenic and chemotactic functions. The antisense oligonucleotide (ASODN) that targets MK has been reported to suppress the growth of tumors in nude mice[11,12]. Additionally,

siRNA or an ASODN that targets MK inhibits neointima formation[13] and renal injury after ischemia[14]. MK has been suggested to play an important role in carcinogenesis, thus MK can serve as a novel tumor marker or therapeutic target.

At present, the delivery tools of siRNAs or ASODNs are ineffective and toxic. Although lentiviral technology is a proven tool in the laboratory setting, it has several adverse effects, such as toxic immune responses and genetic alterations. Therefore, in the present study, we have used the systemic delivery of nanoparticles incorporated with MK-ASODNs (NANO-ASODNs). This delivery approach is a much safer and more effective alternative to viral therapy for the treatment of tumors, such as HCC. NANO-ASODNs have been found to play an important role in the suppression of HCC growth *in vitro* and *in vivo*, and provid insights into their future clinical application to tumor therapy.

MATERIALS AND METHODS

ASODN synthesis

Antisense phosphorothioate oligonucleotide MK-ASODN (5'-CCCCGGGCCGCCCTTCTTCA-3') targeting 108-127 base positions of MK mRNA was synthesized by an Applied Biosystems Model 391 DNA synthesizer (Amersham, Piscataway, NJ, USA) and purified by HPLC (Waters Delta Prep 4000, Milford, MA, USA) using a SOURCE 15Q column (Amersham). In our previous study[15], this antisense sequence has been identified to be the most effective sequence for the down-regulation of MK. Consequently, this sequence was synthesized and applied in this study.

Nanoparticles liposome packageding

Acyl-chloride-cholesterol 2.25 g was dissolved in 5 mL anhydrous chloroform and transferred to a 25-mL three-necked flask. Two milliliters of N', N'-dimethyl-ethanediamine was dissolved into another 5 mL of anhydrous chloroform. The solution was added to the acyl-chloride-cholesterol solution at a constant temperature of 0℃. After dropwise addition, the chloroform was removed by reduction vaporization and the product was purified three times by recrystallization with dehydrated alcohol, and finally eluted with dehydrated alcohol. Following recrystallization, the product was dehydrated by vacuum dehydration for 12 h and the white DC-Chol was obtained. This target product was confirmed by thin-layer chromatography and ^{1}H-NMR exosyndrome analysis. Ten milligrams of DC-Chol and 8 mg of dioleophosphatidyl-ethanolamine were dissolved into chloroform and transferred into a pear shape. The shape was filled with nitrogen gas on a rotary evaporation instrument. Organic solvent was removed by reduction vaporization at a constant temperature of 40℃, until an even lipid film formed on the shape wall. Fifteen milliliter chloroform and 6 mL PBS (pH 7.4) were added into the shape to produce a water-in-oil emulsion adjuvant, using water-bath ultrasound. Chloroform was removed by reduction vaporization on a rotary evaporation instrument to produce a proteoliposome suspension. The suspension was filled with nitrogen gas, made up to a volume of 10 mL with PBS, shattered using a transducer-ultrasound (1 s ultrasound with 2 s breaks for 150 times, with a work rate of 200 W) and filtered using a 0.1-μm polycarbonate membrane five times using a miniextruder. Nanometer liposomes were finally produced. One milliliter of the stock solution (5% manicol) was stored at -70℃ for more than 3 h before vacuum dehydration. The shape and size of the nanometer liposomes were detected by transmission electron microscopy (TEM) and dynamic light scattering.

Cell culture and transduction assay

Human liver HCC cell line HepG2 (HepG2 cells were purchased from the Chinese Academy of Medical Sciences, Beijing, China) were cultured in Dulbecco's Modified Eagle's Medium (DMEM) (Invitrogen Corporation, Carlsbad, CA, USA) supplemented with 10% fetal bovine serum (FBS; GIBCO BRL, Grand Island, NY, USA), 100 U/mL penicillin and 100 μg/mL streptomycin at 37℃ and 5% CO_2. Cells (3×10^3) were seeded in each well of a 96-well microtiter plate and allowed to attach overnight. ASODNs and NANO-ASODNs with different concentrations were added to the cells at different time points. Furthermore, the transduction rate of NANO-ASODNs was analyzed using a confocal microscope (Leica, Heidelberg, Germany).

Cell proliferation assay

NANO-ASODNs with concentrations of 0.1, 0.2, 0.4 and 0.6 μmol/L were added into the HepG2 cell cultures. ASODNs (0.6 μmol/L) transfected into the cells with Lipofectin (Invitrogen), following the manufacturer's instructions, acted as a positive control. Free nanoparticles were added as a negative control. The effects of ASODNs on cellular viability were measured by an MTS [3-(4,5-dimethythiazol-2-yl)-5-(3-carboxymethoxyphenyl)-2-(4-sulfophenyl)-2H-tetrazolium, inner salt] assay. After 48 h of incubation following transfection, 20 μL MTS (Sigma, St Louis, MO, USA) was added to each well and incubated at 37℃ for 2 h. The absorbance values were determined at 490 nm using a MR600 microplate reader (Wallac 1420 Multilable counter; Wallac, Turku, Finland).

In vivo tumor studies

Athymic nude mice (BALB/c-nu/nu females, 6-8 wk old) were purchased from the Academy of Military Medical Science (Beijing, China) and housed in a controlled environment at 22℃ on a 12 h light/12 h dark cycle. Animals were maintained in accordance with the NIH Guide for the Care and Use of Laboratory Animals. The *in situ* HCC models were established as described previously[16]. Three days after the *in situ* HCC models were established, mice were randomly divided into six groups and each experimental group consisted of eight mice. The mice were intravenously injected with PBS (negative control group), 5-fluoro-2, 4 (^{1}H, ^{3}H) pyrimidinedione (5-FU, positive control group) at 10 mg/kg per day and free nanoparticles as a second positive control group. 25, 50 and 100 mg/kg per day of NANO-ASODNs or

free ASODNs were injected into the mice for 20 d. The distribution of NANO-ASODNs was detected with the *in vivo* imaging systems (ICE-FM-1024B, LumazoneFM). Briefly, mice were anesthetized and FAM-NANO-ASODNs or Free ASODNs were intravenously injected through the tail vein. Images were obtained using the YAP-(S) PET scanner (ISE) at 0, 30, 60 and 90 min after injection. The data were acquired in list mode from 256 views over an angle range of 360 degrees. Images were reconstructed using an iterative reconstruction algorithm that provided transaxial, coronal and sagittal slices. At the end of the second *in vivo* imaging study, animals were sacrificed and tumors were removed for radioactivity counting. The body weights of the animals were recorded weekly. Two days after the intravenous injections were completed, mice were sacrificed and the tumors were removed and weighed. Tumor sizes were monitored with calipers; the tumor volume (V, mm^3) was calculated as: V = length × width × depth/2. The percentage of tumor growth inhibition was calculated as: Inhibitory rate = $(W_{control}-W_{treat})/W_{control} \times 100\%$. The blood of the mice was taken for routine blood tests and the α fetoprotein (AFP) test. The tissues of livers and tumors were taken for hematoxylin and eosin (HE) staining and histological examination.

Animal HCC model

The virgin female BALB/c mice used in this experiment were obtained from the Academy of Military Medical Science (Beijing, China). All animal experiments were carried out according to the standards of animal care as outlined in the NIH guide for the Care and Use of Laboratory Animals. The human HCC tumor model was described previously[17]. Briefly, the HCM-Y89 tumor derived from a surgical specimen of HCC was cut into 1 mm × 1 mm × 1 mm pieces, and implanted into the liver of mice. Twenty days later, the mice treated with or without drugs were killed. The tumors were removed and fixed in neutral buffered 10% formalin, processed by standard methods, embedded in paraffin and sectioned and stained with HE. The HCC model maintains various important features similar to clinical liver cancer patients, including local growth, regional invasion, lymph nodes and pulmonary metastasis, peritoneal seeding with bloody ascites, and secretion of AFP in the recipient animals[17].

Histopathological and immunohistochemical analysis

The liver and tumor specimens were fixed and frozen in Tissue Freezing Medium (Triangle Biomedical Sciences, Durham, NC, USA). Five-micrometer sections were cut and stained with HE for histopathological analysis. The immunohistochemical demonstration of anti-MK protein binding was achieved with a rabbit polyclonal anti-MK antibody and an LSAB 2 kit, with visualization of the binding using 3,3'-diaminobenzidine tetrahydrochloride. Staining intensities were classified according to the proportions of positive cells as: negative, none; slightly positive, 50%; positive, 50%-90%; and strongly positive, > 90%. The specificity of the binding was confirmed by negative control staining using a rabbit non-immune serum rather than the primary antibody.

RNA isolation and real-time polymerase chain reaction (PCR)

Total cellular RNA from cell cultures and tissues isolated from the livers and the tumors of mice were extracted using the RNeasy kit according to the manufacturer's protocol. cDNA of the tissue was synthesized from 5 μg of total RNA using a reverse transcription kit. Subsequently, the first strand of cDNA was used as a PCR template. Aliquots of 1 μL of 10-fold diluted cDNA solutions were subjected to PCR in a 20-μL reaction mixture (2 μL PCR buffer; 2 μL dNTP mix; 0.1 μL Taq DNA polymerase; 0.2 μL primers; 14.7 μL autoclaved, distilled water). The primers were as follows: MK, sense primer: 5'-CTCCGCGGTCGCCAAAAAGAAAGA-3'; anti-sense primer: 5'-CCCCCATCACACGCACCCCA GTT-3'. GAPDH, sense primer: 5'-GGAGCCAAAAG GGTCATCATCT-3'; anti-sense primer: 5'-AGGGGCC ATCCACAGTCTTCT-3'. PCR was conducted using a SYBR Premix ExTaqTM kit (TakaRa, Dalian, China) with the following conditions: pre-heating at 95℃ for 2 min, 40 cycles of 30 s denaturation at 94℃, a 20 s annealing at 56℃, and a 40-s extension at 72℃.

Statistical analysis

All parameters were analyzed by analysis of variance. Analysis of variance and Student's *t* test were used to compare each post operative result of each level among all groups. A minimum level of 0.05 was chosen.

RESULTS

Generation of nanoparticles

The produced nanometer liposomes were used to package the MK-ASODNs using a ratio of 1.8 μL of the nanometer liposomes to 1 μg MK-ASODNs (Figure 1A). The nanoparticles packaged with MK-ASODNs were stained with 1% uranyl acetate and examined with an electron microscope. The size of the micelles was determined with a Zetasizer 5000 (Malvern Instruments, Malvern, Worcestershire, UK). The morphology of the nanoparticles packaged with MK-ASODNs was examined using dynamic light scattering and TEM (Figure 1B).

Inhibition of growth of HCC *in vitro*

In order to determine the transduction of NANO-ASODNs, the ASODNs were conjugated with FAM and the rate of transduction under the confocal microscope at different time points was observed. Figure 2A shows that the NANO-ASODNs were effectively transduced into the HepG2 cells at the indicated times (6, 12 and 18 h). Since the NANO-ASODNs readily enter into the cells, we wanted to know whether they could decrease expression of MK in HepG2 cells. Figure 2B shows that the NANO-ASODNs (0.1, 0.2, 0.4 and 0.8 μg/mL) could significantly down-regulate the MK mRNA levels (Figure 2B). The MTS assay was used to analyze the effect of NANO-ASODNs on HCC cell proliferation. Figure 2C shows that the inhibition rates ranged from 20% to 80%, which correlated with the ASODNs concentrations.

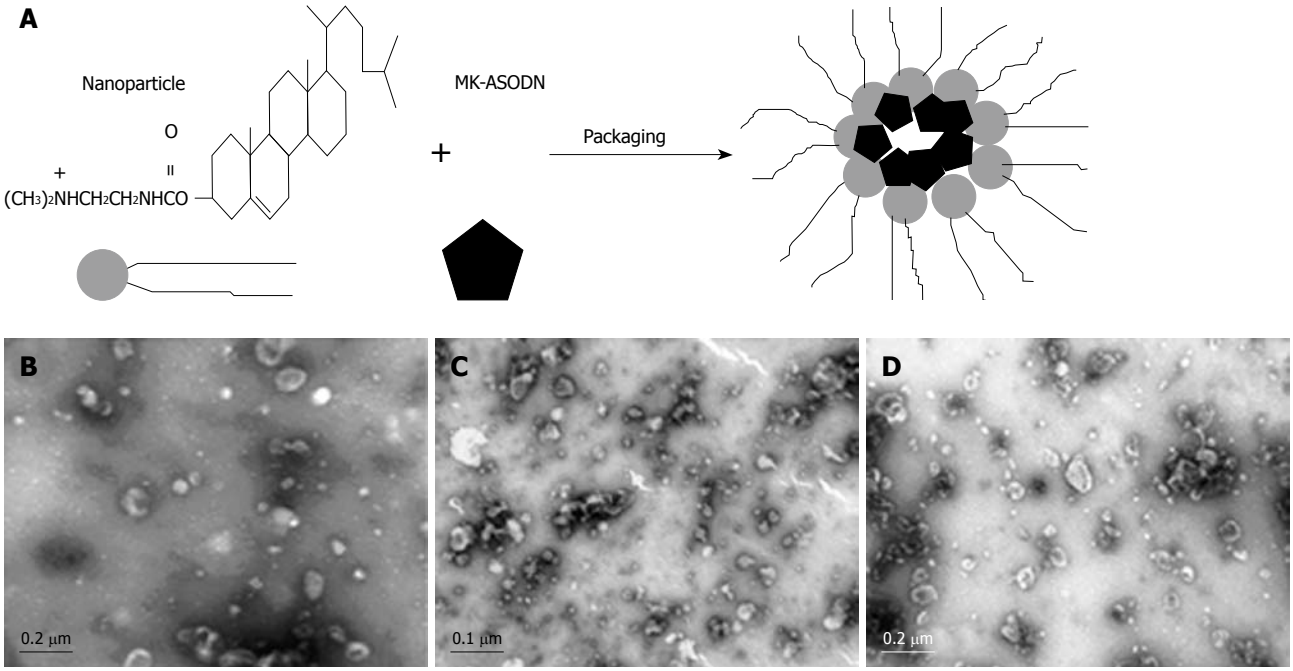

Figure 1 Nano-assembly of MK-ASODNs and nanoliposomes and characterization of NANO-ASODNs. A: Schematic illustration of the self-assembly of MK-ASODN and nanoliposomes; B: TEM image of the empty nanoliposomes stained with 1% uranyl acetate; C, D: TEM image of the NANO-ASODNs.

Table 1 NANO-ASODNs inhibit growth of HCC *in vivo*

Group (mg/kg)	Tumor volume (mm^3)	Tumor weight (g)	Tumor inhibition (%)	AFP (ng/mL)
Control (PBS)	1633.38 ± 525.93	1.92 ± 0.45	-	457.63 ± 141.47
ASODN-100	321.56 ± 85.55[b]	0.57 ± 0.16[b]	70.31	97.63 ± 23.79[b]
ASODN-50	509.29 ± 300.85[b]	0.73 ± 0.22[b]	61.98	179.86 ± 210.27[b]
ASODN-25	835.25 ± 263.33[a]	1.14 ± 0.12[b]	40.63	428.63 ± 141.47
5-FU10	717.19 ± 281.25[b]	0.98 ± 0.16[b]	48.96	315.25 ± 195.77
Nano-ASODN-100	225.81 ± 128.75[b]	0.35 ± 0.17[b]	81.77	58.25 ± 30.83[b]
Nano-ASODN-50	457.88 ± 249.29[b]	0.52 ± 0.21[b]	72.92	89.38 ± 61.75[b]
Nano-ASODN-25	584.00 ± 261.92[b]	0.83 ± 0.20[b]	56.77	205.38 ± 125.16[b]
Nano control	1319.25 ± 340.70	1.59 ± 0.18	17.18	419.25 ± 148.46

[a]$P < 0.05$, [b]$P < 0.01$ *vs* control (PBS).

Inhibition of growth of HCC in vivo

NANO-ASODNs mainly target the liver. In the present study, we used an *in situ* mouse HCC model to evaluate the antitumor activity of NANO-ASODNs. Figure 3 shows that NANO-ASODNs mainly targeted the liver after injection through the tail vein. We also found that the concentration of the NANO-ASODNs reached a peak 90 min after the injection, and then slowly decreased.

Effects of NANO-ASODNs treatment on *in situ* HCC xenograft growth: After establishing the mouse HCC model for 2 d, PBS, free nanoparticles, 10 mg/kg per day 5-FU, various doses of NANO-ASODNs or ASODNs (25, 50 and 100 mg/kg per day) were administered through the tail vein for 20 d. The tumors were removed after sacrificing the mice. The tumors were measured and weighed. Table 1 and Figure 4 show the final tumor volumes and weights after 20 d of treatment. The results showed that the tumor volumes decreased in both free ASODNs and NANO-ASODNs treated groups compared with the PBS control group ($P < 0.01$). Additionally, the effect of NANO-ASODNs on tumor growth inhibition was superior to the free ASODNs ($P < 0.05$). Moreover, the effect of NANO-ASODNs on inhibiting tumor proliferation was dose-dependent (Table 1). In addition, the NANO-ASODNs treatment also resulted in a significant inhibition of tumor weight compared with the PBS- and free-nanoparticle-treated mice. In contrast to the PBS group, it had the highest inhibitory efficacy for the tumor weight which was 81.77% and 10 mg/kg 5-FU had an inhibitory efficacy of 48.96%; however, for the free nanoparticles treatment, the inhibitory rate was only 17.18% ($P < 0.01$) (Table 1).

Histopathological analysis: The morphology of the tumors treated by NANO-ASODNs, ASODNs, 5-FU and PBS were evaluated by HE staining. The tumors were excised at the endpoint of the treatment of each protocol. Figure 5 shows the representative sections of the tumors from each experimental group. The tumors from the mice treated with NANO-ASODNs, ASODNs and 5-FU showed a marked increase in the necrotic

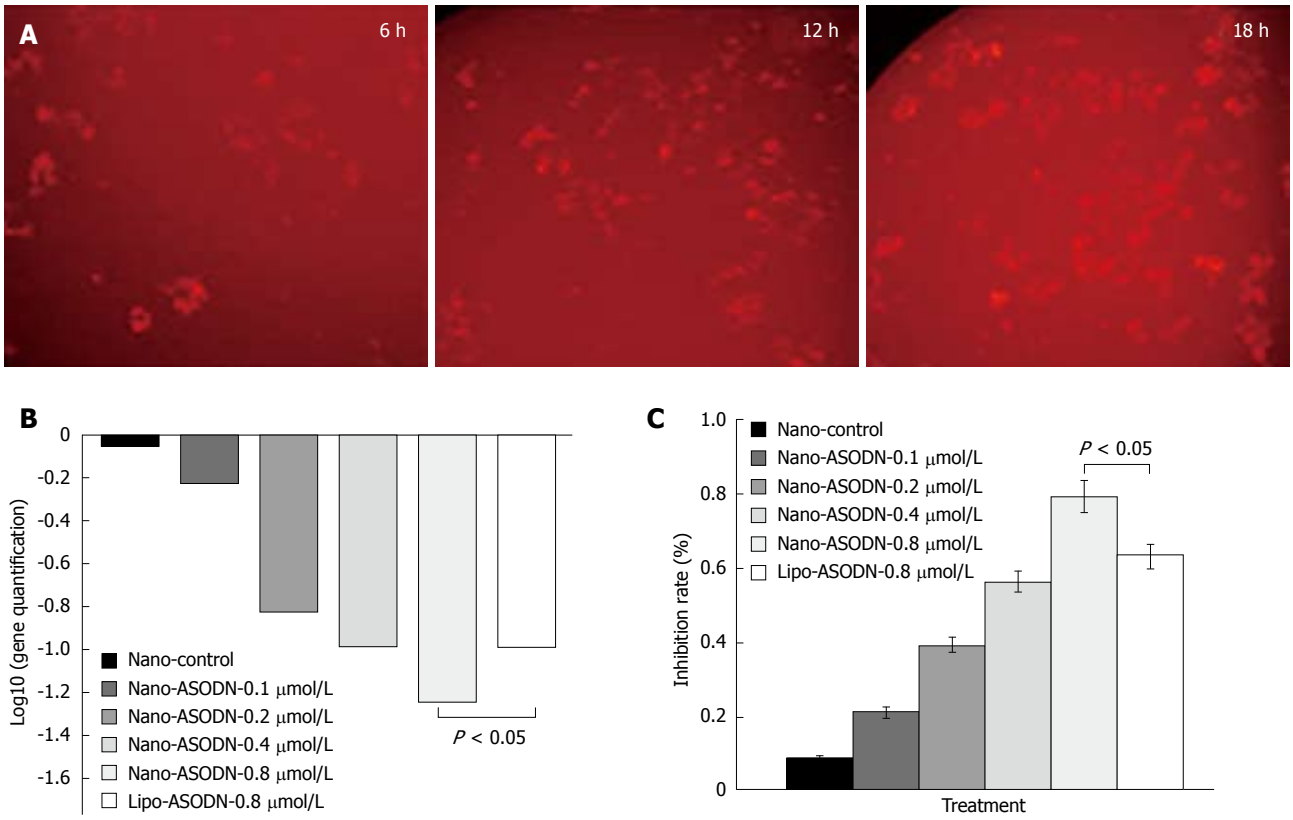

Figure 2 Transduction and function of NANO-ASODNs *in vitro*. A: 0.2 μmol/L FAM-conjugated NANO-ASODNs transduced into HepG2 cells. The results were observed under a confocal microscope at indicted times of 6, 12 and 18 h; B: NANO-ASODNs down-regulated expression of MK mRNA; C: The proliferation of HepG2 cells was significantly inhibited by NANO-ASODNs.

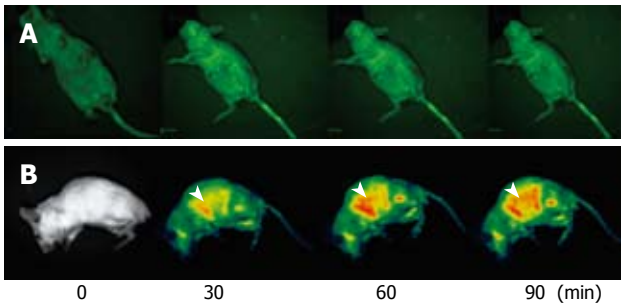

Figure 3 NANO-ASODNs target the liver. The kinetic results of the NANO-ASODNs were observed through *in vivo* imaging systems at indicated times after NANO-ASODNs were injected through the tail vein. A: Free ASODNs did not concentrate within the liver and these ASODNs disappeared quickly; B: NANO-ASODNs were found to mainly target the liver (the arrow represents the NANO-ASODNs).

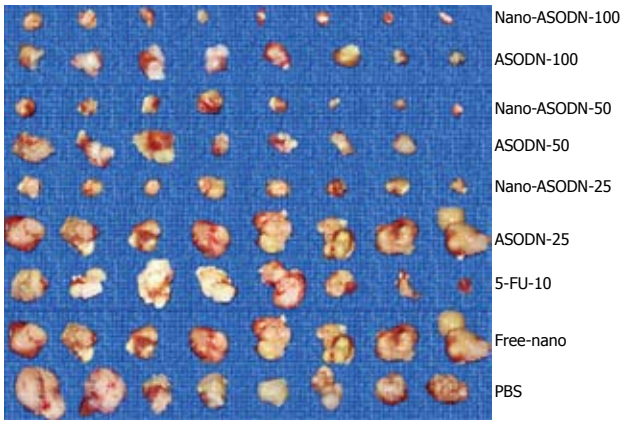

Figure 4 Morphological changes of HCC following treatment with NANO-ASODNs. The volume of HCC decreased significantly following treatment with 100, 50 and 25 mg/kg per day of NANO-ASODNs for 20 d. MK-ASODNs were the positive control. The PBS or free nanoparticles represent the negative controls.

area compared with the PBS-treated animals. This result suggests that the NANO-ASODNs, ASODNs and 5-FU treatment induced HCC necrosis *in vivo*.

Inhibition of plasma AFP secretion: AFP is often expressed in high levels in fetal liver, the gastrointestinal tract and the yolk sack, but AFP is transcriptionally down-regulated after birth and frequently re-expressed in HCC. Therefore, it is often used as an indicator of HCC[18]. In this experiment, we used radioimmunoassay to detect serum AFP concentrations at the endpoint of the treatment. Table 1 shows that NANO-ASODNs at the dose of 100, 50 and 25 mg/kg per day significantly decreased AFP secretion compared with the ASODNs or control groups. This result suggests that there were fewer liver tumor cells in the NANO-ASODNs-treated mice and this treatment reduced circulating AFP.

Systemic toxicity of NANO-ASODNs: Drug treatment of cancer is usually associated with terrible side effects, which result in severe reduction of white blood cell counts or weight loss. In order to evaluate the toxicity of the NANO-ASODNs, we compared the systemic toxicity

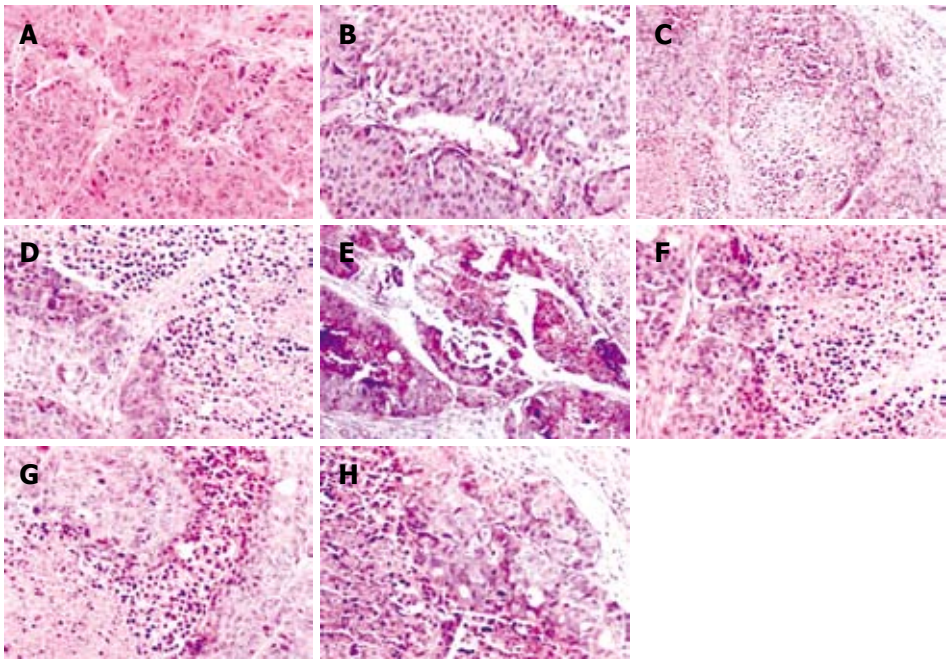

Figure 5 Histopathological analysis. A: Tissue sections of the tumors from *in situ* xenograft HCC; B: Tissue sections of the tumors from nanoparticles; C: Tissue sections of the tumors from 5-FU (10 mg/kg per day); D: Tissue sections of the tumors treated with ASODNs 50 mg/kg per day; E-G: Tissue sections of tumors treated with NANO-ASODNs 100, 50 and 25 mg/kg per day of NANO-ASODN treated tumors, respectively; H: Tissue sections of the tumors treated with 5-FU (10 mg/kg per day) and 50 mg/kg per day of NANO-ASODNs. Regions showing an increase of necrosis and fibrosis were observed in the 5-FU or ASODN treatment groups (C-H, × 200) compared with the free nanoparticles and untreated groups (A and B, × 200).

of free ASODNs, 5-FU and NANO-ASODNs. Mice without tumors were administered a dose of 10 mg/kg per day ASODNs, 5-FU and NANO-ASODNs, and PBS as the control. The body weight was subsequently monitored. The results showed that the mean body weight decrease of the NANO-ASODNs group was not significantly different compared with the ASODNs or PBS groups ($P > 0.05$). However, the decrease in the weight of ASODN- and 5-FU-treated mice was more significant (data not shown). In addition, no inflammatory infiltrate was observed surrounding the solid tumor after treatment with different concentrations of the NANO-ASODNs (data not shown).

All the above studies suggest that nanoparticles packaged with ASODNs were safer than free ASODNs or chemical drugs.

DISCUSSION

MK is a heparin-binding growth factor identified as a product of a retinoic acid response gene[19,20]. MK is overexpressed in a wide range of human carcinomas and believed to contribute to tumorigenesis and tumor progression. HCC is the most common primary liver malignancy, with a rising incidence worldwide. At present, although surgery and chemotherapy are effective in patients with localized tumors, the prognosis of patients with advanced or metastatic tumors is not ideal. Therefore, novel treatment approaches for the cancer are urgently needed. Recently, HCC tumor cells were found to overexpress MK. In our previous studies, ASODNs that target MK were demonstrated to play an important role in anti-tumor functions[15,16]. However, the anti-tumor effect was not satisfactory and found to be toxic because of the absence of smart and safer delivery tools. At present, the strategies that have been adopted to improve the uptake of various nucleic-acid-based therapeutic agents are microinjection, passive diffusion, endocytosis (i.e. receptor mediated endocytosis, fluid phase pinocytosis, adsorptive endocytosis) and artificially enhanced uptake (i.e. using delivery vectors like liposomes, micro- or nanoparticles or dendrimers)[21,22].

In the present study, we used more effective and less toxic nanoparticle liposomes that have previously been used effectively to deliver siRNA for the treatment of lymphoma and ovarian cancer, as well as colorectal carcinoma. Liposomes, the first nanotechnology to benefit cancer patients, are continuing to evolve as tools for delivering potentially useful therapies for the treatment against tumors. In this study, MK-ASODNs incorporated into nanoliposomes have been used effectively *in vivo*. Evidence from these experiments showed that nanoliposomes packaged with MK-ASODNs could suppress HCC growth both *in vitro* and *in vivo*. In addition, the data also indicated that nanoliposomes could effectively deliver MK-ASODNs and showed less systematic toxicity. Consequently, nanoliposomes incorporated with MK-ASODNs should represent an effective and less toxic approach for treatment of HCC, and potentially, other tumor types.

In summary, our results suggest that nanoliposomes packaged with MK-ASODNs can increase the therapeutic effect of MK-ASODNs, both *in vivo* and *in vitro*, for the treatment of HCC. The combination of nanoliposomes and MK-ASODNs showed a more effective and less toxic tool for therapy against HCC and should provide a novel strategy for cancer treatment.

COMMENTS

Background

Midkine (MK) is a 13-kDa protein with a heparin-binding growth factor function. MK has been found to play important roles in carcinogenesis, including mitogenic, anti-apoptotic, transforming, fibrinolytic, chemotactic and angiogenic cancer-related activities.

Research frontiers

MK plays an important role in tumor development and progression.

Nanoliposomes packaged with MK-antisense oligonucleotides (ASODNs) can inhibit growth of hepatocellular carcinoma (HCC), both *in vitro* and *in vivo*, and potentially represents a significant clinical benefit.

Innovations and breakthroughs

In this study, nanoliposomes effectively delivered MK-ASODNs *in vitro* and *in vivo* with low toxicity. Additionally nanoliposomes packaged with MK-ASODNs inhibited proliferation of HepG2 cells and the growth of HCC xenografts.

Applications

In this study, the authors addressed the potential therapeutic effect of nanoliposomes packaged with MK-ASODNs on the suppression of HCC growth. Significant inhibition of HCC growth was achieved using the nanoliposomes packaged with MK-ASODN. This observation indicates that the nanoliposomes packaged with MK-ASODN are an effective anti-tumor agent.

Terminology

MK is a growth protein, which is overexpressed in HCC and promotes the growth of tumors. Nanoparticles represent powerful delivery tools, which can effectively deliver drugs or molecules into cells.

Peer review

The authors studied the growth inhibition of HCC *in vitro* and *in vivo* with nanoparticles delivering MK-ASODNs. MK-ASODNs have been shown to inhibit the growth of HCC. They found that the proliferation of HepG2 cells was significantly inhibited in the presence of different concentrations of nanoparticles packaged with MK-ASODNs (NANO-ASODNs). Furthermore, in the HCC mouse model, the NANO-ASODNs mainly accumulated in the liver and significantly inhibited the growth of the HCC tumors.

REFERENCES

1 **Yang L**, Parkin DM, Ferlay J, Li L, Chen Y. Estimates of cancer incidence in China for 2000 and projections for 2005. *Cancer Epidemiol Biomarkers Prev* 2005; **14**: 243-250

2 **Parkin DM**, Bray F, Ferlay J, Pisani P. Global cancer statistics, 2002. *CA Cancer J Clin* 2005; **55**: 74-108

3 **Michikawa M**, Xu RY, Muramatsu H, Muramatsu T, Kim SU. Midkine is a mediator of retinoic acid induced neuronal differentiation of embryonal carcinoma cells. *Biochem Biophys Res Commun* 1993; **192**: 1312-1318

4 **Garver RI Jr**, Radford DM, Donis-Keller H, Wick MR, Milner PG. Midkine and pleiotrophin expression in normal and malignant breast tissue. *Cancer* 1994; **74**: 1584-1590

5 **Take M**, Tsutsui J, Obama H, Ozawa M, Nakayama T, Maruyama I, Arima T, Muramatsu T. Identification of nucleolin as a binding protein for midkine (MK) and heparin-binding growth associated molecule (HB-GAM). *J Biochem* 1994; **116**: 1063-1068

6 **Aridome K**, Tsutsui J, Takao S, Kadomatsu K, Ozawa M, Aikou T, Muramatsu T. Increased midkine gene expression in human gastrointestinal cancers. *Jpn J Cancer Res* 1995; **86**: 655-661

7 **Nakanishi T**, Kadomatsu K, Okamoto T, Tomoda Y, Muramatsu T. Expression of midkine and pleiotropin in ovarian tumors. *Obstet Gynecol* 1997; **90**: 285-290

8 **O'Brien T**, Cranston D, Fuggle S, Bicknell R, Harris AL. The angiogenic factor midkine is expressed in bladder cancer, and overexpression correlates with a poor outcome in patients with invasive cancers. *Cancer Res* 1996; **56**: 2515-2518

9 **Konishi N**, Nakamura M, Nakaoka S, Hiasa Y, Cho M, Uemura H, Hirao Y, Muramatsu T, Kadomatsu K. Immunohistochemical analysis of midkine expression in human prostate carcinoma. *Oncology* 1999; **57**: 253-257

10 **Mishima K**, Asai A, Kadomatsu K, Ino Y, Nomura K, Narita Y, Muramatsu T, Kirino T. Increased expression of midkine during the progression of human astrocytomas. *Neurosci Lett* 1997; **233**: 29-32

11 **Takei Y**, Kadomatsu K, Matsuo S, Itoh H, Nakazawa K, Kubota S, Muramatsu T. Antisense oligodeoxynucleotide targeted to Midkine, a heparin-binding growth factor, suppresses tumorigenicity of mouse rectal carcinoma cells. *Cancer Res* 2001; **61**: 8486-8491

12 **Takei Y**, Kadomatsu K, Goto T, Muramatsu T. Combinational antitumor effect of siRNA against midkine and paclitaxel on growth of human prostate cancer xenografts. *Cancer* 2006; **107**: 864-873

13 **Johnson PJ**. The role of serum alpha-fetoprotein estimation in the diagnosis and management of hepatocellular carcinoma. *Clin Liver Dis* 2001; **5**: 145-159

14 **Banno H**, Takei Y, Muramatsu T, Komori K, Kadomatsu K. Controlled release of small interfering RNA targeting midkine attenuates intimal hyperplasia in vein grafts. *J Vasc Surg* 2006; **44**: 633-641

15 **Dai LC**, Wang X, Yao X, Lu YL, Ping JL, He JF. Antisense oligonucleotides targeting midkine induced apoptosis and increased chemosensitivity in hepatocellular carcinoma cells. *Acta Pharmacol Sin* 2006; **27**: 1630-1636

16 **Dai LC**, Wang X, Yao X, Min LS, Ping JL, He JF. Antisense oligonucleotides targeting midkine inhibit tumor growth in an in situ human hepatocellular carcinoma model. *Acta Pharmacol Sin* 2007; **28**: 453-458

17 **Lin RX**, Tuo CW, Lü QJ, Zhang W, Wang SQ. Inhibition of tumor growth and metastasis with antisense oligonucleotides (Cantide) targeting hTERT in an in situ human hepatocellular carcinoma model. *Acta Pharmacol Sin* 2005; **26**: 762-768

18 **Sato W**, Takei Y, Yuzawa Y, Matsuo S, Kadomatsu K, Muramatsu T. Midkine antisense oligodeoxyribonucleotide inhibits renal damage induced by ischemic reperfusion. *Kidney Int* 2005; **67**: 1330-1339

19 **Nakagawara A**, Milbrandt J, Muramatsu T, Deuel TF, Zhao H, Cnaan A, Brodeur GM. Differential expression of pleiotrophin and midkine in advanced neuroblastomas. *Cancer Res* 1995; **55**: 1792-1797

20 **Tsutsui J**, Kadomatsu K, Matsubara S, Nakagawara A, Hamanoue M, Takao S, Shimazu H, Ohi Y, Muramatsu T. A new family of heparin-binding growth/differentiation factors: increased midkine expression in Wilms' tumor and other human carcinomas. *Cancer Res* 1993; **53**: 1281-1285

21 **Dai H**, Jiang X, Tan GC, Chen Y, Torbenson M, Leong KW, Mao HQ. Chitosan-DNA nanoparticles delivered by intrabiliary infusion enhance liver-targeted gene delivery. *Int J Nanomedicine* 2006; **1**: 507-522

22 **Elouahabi A**, Ruysschaert JM. Formation and intracellular trafficking of lipoplexes and polyplexes. *Mol Ther* 2005; **11**: 336-347

S- Editor Li LF **L- Editors** Ma JY and Kerr C **E- Editor** Lin YP